Original paper

The role of peridotite and pyroxenite melts in the origin of the Karapınar basalts, Cappadocia Volcanic Province, Central Anatolia

Gülin GENÇOĞLU KORKMAZ[1]*, Hüseyin KURT[1], Kürşad ASAN[1], Maurizio PETRELLI[2], Matthew LEYBOURNE[3]

[1] *Department of Geological Engineering, Faculty of Engineering and Natural Sciences, Konya Technical University, 42250 Konya, Turkey; ggkorkmaz@ktun.edu.tr*
[2] *Department of Physics and Geology, University of Perugia, 06123 Perugia, Italy*
[3] *Queen's University Department of Geological Sciences and Geological Engineering, K7L 3N6, Kingston, Ontario, Canada*
[*] *Corresponding author*

This study investigates the mantle source characteristics of the Quaternary Karapınar Basalts from the southwestern part of the Cappadocia Volcanic Province (CVP) in Central Anatolia using a combination of whole-rock and olivine major- and trace-element geochemistry as well as olivine oxygen isotope composition. Petrographic features and trace element distributions demonstrate that the Karapınar basalts can be classified into two sub-groups as basalt-1 (KB1/alkaline–calc-alkaline) and basalt-2 (KB2/calc-alkaline). Although these two types of basalts are petrographically, texturally and geochemically different, they exhibit similar "orogenic type" incompatible trace element patterns in MORB-normalized diagrams. KB1 basalts are relatively primitive (e.g., up to 12 wt. % MgO) and calc-alkaline to mildly alkaline (Ne-normative content up to 5 %) in character, whereas KB2 basalts are enclave-bearing, calc-alkaline (hypersthene-normative plus quartz or olivine) ones with the more evolved composition. The most primitive olivine from the KB1 exhibits normal zoning, from core compositions of Fo_{89} to rim compositions of $Fo_{86,}$ with a concomitant decreasing in Ni and increasing MnO and CaO contents. On the contrary, the KB2 olivines show both inverse and normal zoning in terms of CaO and MnO contents. Moreover, the studied olivine phenocrysts have enriched rims and/or growth zones in Li, Zn, Cr, Ti, Sc, and V contents, which indicates a source containing recycled continental crust and/or magma recharging processes. The olivine from the most primitive samples (KB1; MgO > 10 wt. %) has high Zn/Fe, Fe/Mn, Co, Zn, Ni, Ca, and low Mn/Zn, Co/Fe values indicating melt addition from a pyroxenitic source. Calculations based on the olivine chemistry indicate that the most primitive nepheline normative KB1 rocks originated from the melting of mixed pyroxenitic-peridotitic source that shows the average proportion of ~70 % and ~30 %, respectively. The mean $\delta^{18}O$ values of olivine phenocrysts (+6.4 ‰; n = 8) from the Karapınar basaltic rocks are higher than typical mantle olivine (+5.1–5.4 ‰) but overlap known OIB-EMII sources (+5.4–6.1 ‰). Collected data indicate that the Karapınar basalts are the mixing products of partial melts from mantle peridotite and metasomatic pyroxenite generated by the reaction of the subducted oceanic slab-derived melts with the surrounding peridotite, related to the convergence system of the Eurasian and Afro–Arabian plates.

Keywords: Karapınar Basalt, olivine, oxygen, peridotite, pyroxenite, source
Received: 10 February 2022; accepted: 8 October 2022; handling editor: F. Tomek
The online version of this article (doi: 10.3190/jgeosci.362) contains supplementary electronic material.

1. Introduction

Peridotites have been generally known as the main source lithology for basaltic magmas (e.g., Green and Ringwood 1967; McKenzie and Bickle 1988). However, recent experimental studies reveal that pyroxenite or its mixture with peridotite was considered the presumable source lithology of some alkaline basalts (Kogiso et al. 2003; Sobolev et al. 2007; Dai et al. 2018). Pyroxenite is known as an ultramafic igneous rock consisting actually of minerals of the pyroxene group and is not found as common as peridotite in the upper mantle. Recent studies clearly exhibited that pyroxenite could be occurred by reaction of recycled oceanic crust-derived melts with the surrounding mantle peridotite via exhausting olivine and producing pyroxene (e.g., Kogiso et al. 2003; Sobolev et al. 2007; Herzberg 2011; Zhang et al. 2019). They may be involved in various petrogenetic processes, such as the genesis of mid-ocean ridge basalts (MORBs; Hirschmann and Stolper 1996; Zhang et al. 2012) and within plate magmas (Sobolev et al. 2005; Pilet et al. 2008). Unraveling the petrogenesis of mantle-derived melts is quite difficult and complex. The potential mantle temperature (Tp; McKenzie and O'Nions 1991), the thickness of the lithosphere, and the volume of recycled oceanic crust in the upwelling mantle, which are the key parameters for the interpretation of the magma genesis, must be accounted for the determination and the restric-

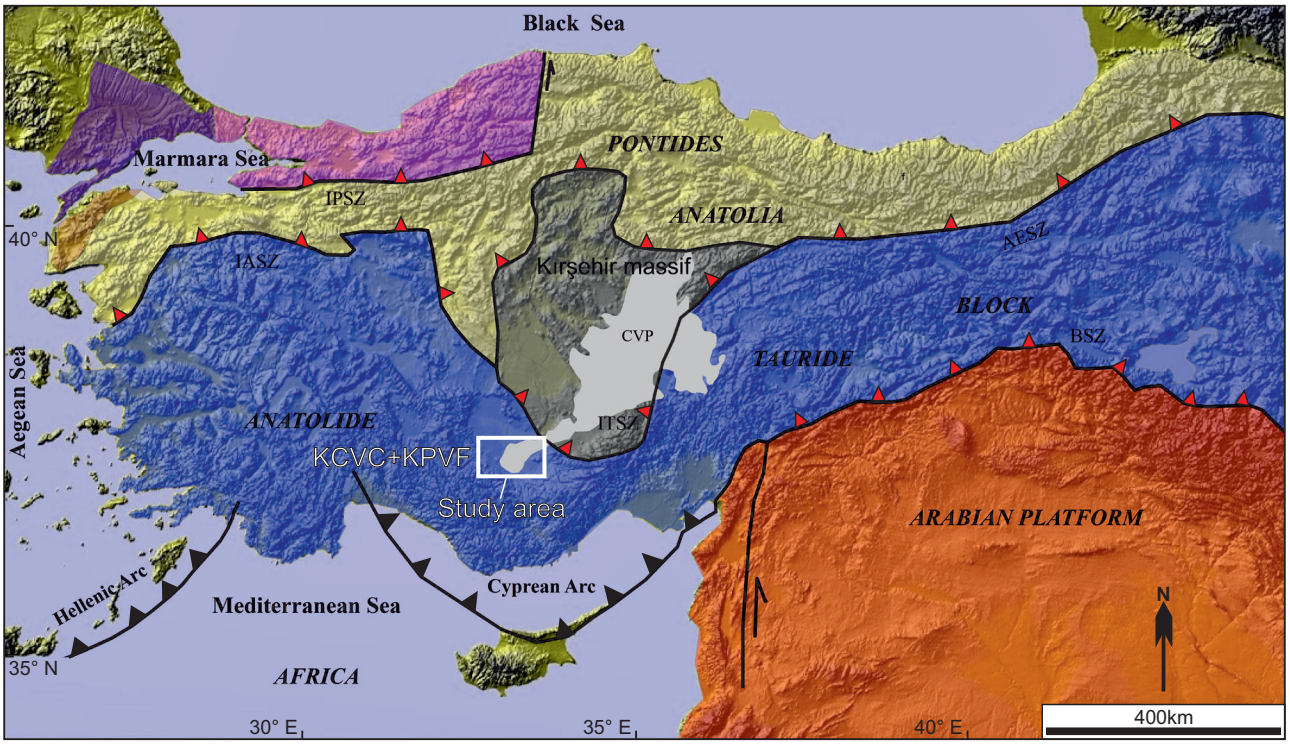

Fig.1 (a) Location map of the investigated area taken from Gençoğlu Korkmaz et al. (2022). The map displays the main tectonic units of Turkey (Okay and Tüysüz 1999). IASZ: Izmir-Ankara-Suture Zone, AESZ: Ankara-Erzincan Suture Zone, IPSZ: Intra-Pontide Suture Zone, ITSZ: Inner Tauride Suture Zone, BSZ: Bitlis Suture Zone, CVP: Cappadocian Volcanic Province. Black lines with red triangles represent major suture zones and black lines with filled triangles represent arc systems.

tion of the magma source lithology (Sobolev et al. 2007). For instance, at constant Tp, pyroxenite starts to partially melt at a higher pressure than peridotite (Yaxley 2000). Therefore, a thick lithosphere will give rise to a higher proportion of pyroxenite- than peridotite-derived partial melts (Morgan 2001; Ito and Mahoney 2005). Moreover, several late-stage processes such as melt differentiation, magma mixing, and crustal contamination modify the elemental as well as the isotopic signature of these magmas during their transport to the surface (Sobolev et al. 2005, 2007; De Hoog et al. 2010; Gurenko et al. 2010; Le Roux et al. 2010; Herzberg 2011; Zhang et al. 2012; Foley et al. 2013; Herzberg et al. 2014; Guo et al. 2015; Søager et al. 2015). Therefore, to understand and evaluate the source characteristics of magmas, the composition of unaltered olivine could serve as a powerful record of the history of the petrogenetic processes because it generally represents the first-crystallized phase (Søager et al. 2015). Consequently, petrogenetic studies mainly focus on primitive magmas (i.e., unaltered basalts characterized by high Mg#) and unaltered olivine or pyroxene grains (Sobolev et al. 2005, 2007; De Hoog et al. 2010; Gurenko et al. 2010; Le Roux et al. 2010; Herzberg 2011; Zhang et al. 2012; Foley et al. 2013; Herzberg et al. 2014; Guo et al. 2015; Søager et al. 2015). For example, to constrain the involvement of pyroxenite rocks in the petrogenesis of primitive magmas, Sobolev et al. (2005) and Sobolev et al. (2007) investigated the trace element systematics of olivine, and they performed several batch-melting experimental studies to calculate the involvement of pyroxenite- and peridotite derived melt in the petrogenesis of komatiite, ocean island basalt, mid-ocean ridge basalt, and continental basalt. Their studies were based on the supposition that a hybrid pyroxenitic source formed by the reaction of eclogitic melt with peridotite in the asthenospheric mantle during subduction. In order to evaluate the amount of eclogite-derived melt needed to produce hybrid pyroxenite from peridotite and the actual amount of recycled material in the source, they recommended a relative proportion of degree of melting of eclogite (50 %), pyroxenite (50 %), and peridotite (10–20 %); for MORB, within plate basalt on thick > 70 km lithosphere and thin lithosphere < 70 km.

Recently, there has been a significant debate regarding the source lithology of the Quaternary-aged mafic volcanic rocks from the Cappadocia Volcanic Province (CVP) in Central Anatolia. Some of the previous studies suggest that alkaline basaltic rocks from the southern part of the CVP stemmed from the spinel lherzolitic source, whereas others claim that a single-homogenous spinel lherzolitic source is not adequate for generating the liquids for the formation of the alkaline basalts (Kürkcüoğlu and Yürür 2022).

Here, we provide the first time olivine major and trace element data as well as olivine $\delta^{18}O$ isotope compositions and new bulk-rock geochemical data for Quaternary aged post-collisional Karapınar basaltic rocks from the southwestern part of the Cappadocia Volcanic Province (CVP) in Central Anatolia, Turkey to interpret the chemical heterogeneity of the mantle sources. Two geochemical types represent the Karapınar basalts; KB1 is transitional (mildly alkaline to calc-alkaline), high-MgO basalt (>10 % MgO) with primitive olivine (Mg# of 88–89; Matzen et al. 2017), and KB2 is calc-alkaline, evolved basalt including lower Mg# of olivine. The study's main aim is to understand and evaluate the petrogenetic evolution of the Karapınar basalts, mainly focusing on the possible involvement of pyroxenitic melts in the source and their later evolution in the crustal levels. Therefore, we have used the whole-rock and olivine chemistry of KB1 to constrain mantle source characteristics and those of KB2 to reveal crustal magma chamber processes throughout this paper.

2. Regional geology and volcanism

Anatolia (Turkey, Eastern Mediterranean) is a region situated between the Africa-Arabian and the Eurasian plates, and includes several tectonic units accreted during the closure of the various branches of the Neotethys Ocean (Fig. 1; Şengör and Yılmaz 1981; Okay and Tüysüz 1999). The Southern Branch of the Neotethys Ocean was fully subducted in the east (Şengör et al. 2003), even though subduction is still active today in the western part, and it is likely related to slab roll-back and slab break-off processes from the Middle Miocene onwards (Faccenna et al. 2006; van Hinsbergen et al. 2010; Biryol et al. 2011; Gençoğlu Korkmaz et al. 2017; Asan et al. 2021). It is stated that an uplift in Central Anatolia since the Middle Miocene may have resulted from the retreating of the subduction of the Neo-Tethyan plate and delamination of the mantle lithosphere (Bartol and Govers 2014), the collapse of the mantle lithosphere (Göğüş et al. 2017), or the dynamic uplift of the asthenospheric mantle (Faccenna and Becker 2010). Moreover, Boschi et al. (2010) and Faccenna and Becker (2010) suggest that the dynamic response to underlying mantle heterogeneities may have an important role in the occurrence of the high elevations in the region. The main governing processes responsible for the formation of the Central Anatolian Basin are tectonism, volcanism, and sedimentation for the period of Late Miocene to Late Quaternary. Faulting controlled the site of the volcanoes within the CVP. Hence from the Miocene to historical times, it produced widespread subduction-related volcanism in Central Anatolia (Şengör and Yılmaz 1981; Toprak 1998). From the Miocene to the present, Cappadocian volcanoes have occurred as both stratovolcanoes and monogenic edifices producing both basaltic and evolved volcanic rocks (Aydar et al. 1994). The CVP is mainly composed of the Mio-Pliocene calc-alkaline, andesitic-dacitic to rhyolitic lava flows, domes, and related pyroclastic products (Innocenti et al. 1975; Notsu et al. 1995; Deniel et al. 1998; Kürkçüoğlu et al. 1998; Temel et al. 1998; Gençalioğlu Kuşçu and Geneli 2010). However, Quaternary volcanism in the area mainly produced mildly alkaline to alkaline basaltic lava flows, scoria cones and maars (Ercan 1987; Aydar et al. 1994; Gençalioğlu-Kuşcu et al. 2007; Aydın et al. 2014; Uslular et al. 2015; Dogan-Kulahci et al. 2018). The chemical (i.e., major and trace element) signature and isotopic composition (i.e., Sr-Nd-Pb) indicate that assimilation of crustal materials had a key role in the formation of the CVP (Innocenti et al. 1975; Ercan 1987; Pasquarè et al. 1988; Ercan et al. 1990; Aydar et al. 1994; Notsu et al. 1995; Deniel et al. 1998; Aydın et al. 2014; Di Giuseppe et al. 2018; Dogan-Kulahci et al. 2018). In contrast to Western and Eastern Anatolia, the mildly-alkaline basaltic volcanic activity postdating and/or being coeval with the orogenic calc-alkaline one is characterized by orogenic geochemical signatures in Central Anatolia (Ercan et al. 1990; Di Giuseppe et al. 2018 ; Reid et al. 2017; Dogan-Kulahci et al. 2018). This different signature in the CVP basalts has recently been attributed to either a mixing process between subduction-related calc-alkaline and within-plate OIB-like magmas, close to their source area (Di Giuseppe et al. 2018) or crustal contamination (Gençoğlu Korkmaz et al. 2022) of parental melts during ascent.

The Karacadağ Volcanic Complex (KCVC) and Karapınar Volcanic Field (KPVF) are located on the southwestern edge of the CVP in Central Anatolia (Fig. 1; Gençoğlu Korkmaz et al. 2022). Mainly intermediate-felsic volcanic rocks accompanied by scarce mafic rocks, both of Neogene age, are represented by the products of lava flows and domes; the "KCVC". While, Quaternary mafic to intermediate volcanic rocks of KPVF are represented by the scoria cones, lava flows, dykes, and maars (Gençoğlu Korkmaz et al. 2022). The KPVF rocks overlie the KCVC rocks in the region (Keller 1974). Previous studies yielded an age of 2.5 Ma (Ar–Ar) for the KPVF (Reid et al. 2017; Dogan-Kulahci et al. 2018), while K–Ar and Ar–Ar geochronology yield 4.7 to 6.0 Ma age span for the KCVC (Platzman et al. 1998; Gençoğlu Korkmaz et al. 2022). Moreover, the previous studies (Kurt et al. 2019; Gençoğlu Korkmaz and Kurt 2021) reported that decompression and multiple/repeated recharging events had a crucial role in the evolution of the KCVC and KPVF.

Recent geophysical and thermal studies (Reid et al. 2017; McNab et al. 2018; Artemieva and Shulgin 2019)

indicate that the lithospheric thickness of Central Anatolia is not uniform. Artemieva and Shulgin (2019) suggest that the non-uniform lithosphere structure beneath the Central Anatolian Plateau with lithosphere thickness variations from more than 150–175 km to ca. 50 km depth. Also, the belt of the thin lithosphere in Central Anatolia coincides to a linear belt of the Neogene volcanoes where mantle melting at ca. 60–80 km depth may be expected.

3. Sampling and analytical methods

The most representative and freshest rocks from the Karapınar basaltic rocks were collected in the Karapınar area, Konya. Petrography of basaltic rock samples (KB1, KB2) and their enclaves (MME: Mafic magmatic enclave) was performed using a polarizing microscope at the Geological Engineering department mineralogy labs of the Konya Technical University. Then, the representative and freshest thirteen samples, showing little or no alteration, were analyzed at the Ankara University, Earth Sciences Application and Research Center (YEBİM) laboratory (Ankara, Turkey) for major/trace element contents by X-Ray Fluorescence Spectrometry using Spectro X-LAB 2000. The samples were crushed in a Retsch brand automatic rock crusher and then ground in a tungsten carbide mill in a FRITSCH brand automatic grinder. Afterward, ~4 g of powdered sample was mixed with 0.9 g of binder comprised of wax and compressed to produce a powder pellet for subsequent analyses. Moreover, we utilized some of our published whole-rock data (five samples; Gençoğlu Korkmaz et al. 2022) to strengthen our new model. All major and trace elements analyzed are given in Supplementary Tab. S1.

The representative fourteen olivine grains from KB1, KB2, and MME were selected to obtain a general overview of the chemical variation of major oxides. Major element analyses of olivines were performed at the YEBİM by electron probe microanalysis (EPMA). Thin sections were polished and coated with carbon and analyses were performed using a JEOL JXA 8230 EPMA under 20 kV voltage and 15 nA current. A detailed description of the analytical protocol for EPMA determinations is reported by Deniz and Kadıoğlu (2019).

Eight representative olivine grains were selected, and their trace element compositions were determined by laser ablation inductively coupled mass plasma spectrometry (LA–ICP–MS) technique at the Department of Physics and Geology, Perugia University (Italy). The analyses were performed using a Thermo Fisher Scientific iCAP ICP–MS coupled with Teledyne Photon Machine G2 laser ablation system using helium as the carrier gas. In order to boost the instrumental sensitivity and avoid plasma destabilization, N_2 and Ar were added, respectively. The conditions used were: repetition rate of 8 Hz, fluence of 3.5 J/cm^2, 25 μm spot size and dwell time of 10 ms. Single spot measurements were executed on the rims, growth zones and cores of olivine crystals showing diverse textures, zoning patterns and compositions. Data were gathered for Al, Li, Ca, Na, P, Sc, Co, Ti, Cr, V, Zn, Mn, Zr, Ni, Nb, and Y. The USGS BCR–2G glass was used for quality control, while NIST 610 was utilized for the calibration. As an internal standard, Si compositions acquired by EPMA analyses were used. The Iolite v.3 software was used for data reduction (Paton et al. 2011). The accuracy and precision of the analyses were better than 10 % (see Petrelli et al. 2008, 2016a, b). Repeated analyses (n = 6) of the USGS BCR2G reference material executed in the same analytical session of the data mentioned in the present study approved the anticipated figures of merits. All major oxide and trace element data of olivine are given in Tab. S1. In this study, to detect and evaluate the source area and constrain the source lithology, we utilized the mineral chemistry data of olivine phenocrysts from the most primitive basalts (MgO > 10 wt. %), which gives the most accurate knowledge regarding the mantle source compositions.

The eight basaltic rocks (KB1, KB2, and MME) were measured at the Queen's Facility for Isotope Research (QFIR) laboratory (Queen's University, Canada) for $\delta^{18}O$ stable isotope analysis. The $^{18}O/^{16}O$ ratios of separated olivine minerals were carried out by Thermo-Finnigan Delta Plus XP Isotope-Ratio Mass Spectrometer (IRMS), following the liberation of O_2 by BrF_5 reaction in Ni vessels and conversion to CO_2. All results are calibrated to certified VSMOW, VSLAP9 reference materials and reported in standard permil notation (‰). The accuracy of the analyses was 0.5‰. A detailed description of the analytical protocol for $\delta^{18}O$ stable isotope analysis determinations is reported by Gençoğlu Korkmaz et al. (2022). Stable isotope analyses of the samples are reported in the Tab. S1.

4. Results

4.1. Petrography and classification of the volcanics

The petrographic and chemical features of the investigated volcanic suite indicate that the Karapınar basaltic rocks can be discriminated into two sub-groups; basalt-1 (KB1) and basalt-2 (KB2). The KB1 group rocks have holo-to hypocrystalline porphyritic texture and are comprised of mainly olivine and plagioclase, with lesser clinopyroxene, and Fe–Ti-oxide microphenocrysts in an intergranular to intersertal groundmass (Figs 2a, 2b). Olivine and clinopyroxene phenocrysts are generally

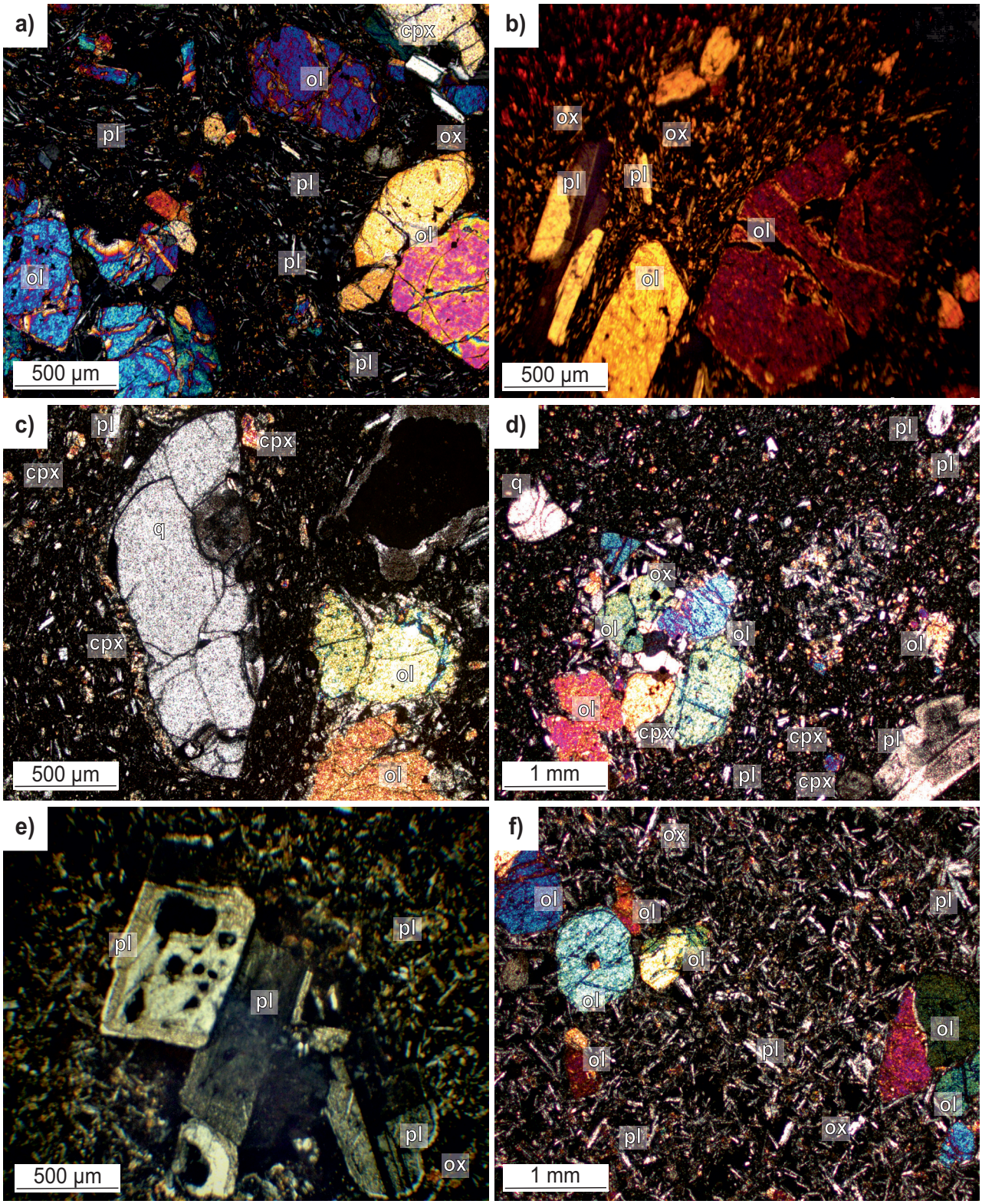

Fig. 2. Petrography of the studied basaltic rocks from the Karapınar. (a) Euhedral–subhedral-shaped olivine and (b) euhedral–subhedral-shaped olivine and plagioclase phenocrysts in the KB1 group rocks. (c) Embayed and ocelli quartz xenocryst and (d) olivine crystal clots and sieved-plagioclase in the KB2 group rocks. (e) Sieved-plagioclase glomerocrysts and (f) basaltic mafic magmatic enclaves and relatively rounded olivines in the KB2 group rocks. (cpx: clinopyroxene; ol: olivine; ox: Fe–Ti oxide; pl: plagioclase; q: quartz).

euhedral-subhedral. Olivine rarely shows skeletal textures and iddingsitization. By contrast, the KB2 group rocks are holo- to hypo-crystalline porphyritic, also exhibit vesicular texture and rarely include amygdales filled with carbonate and siliceous material. The KB2 rocks generally have clinopyroxene and plagioclase phenocrysts, and rare olivine microcrysts and phenocrysts (Figs 2c–2e). The groundmass is composed of the same mineral phases plus Fe–Ti oxide minerals and some glass. KB2 group rocks also have xenocrysts of plagioclase, biotite and rounded, embayed, and ocelli-quartz (Fig. 2c), as well as plagioclase glomerocrysts (Fig. 2e). Olivine in KB2 rocks are generally subhedral-anhedral and rounded (Figs 2c–2f). Plagioclase xenocrysts commonly exhibit sieve textures (fine-coarse-dusty sieve; Figs 2d,e). Some of the investigated rocks contain olivine ± clinopyroxene crystal clots (Fig. 2d), and mafic magmatic enclaves (MME) whose olivine are rarely anhedral and generally rounded and fractured (Fig. 2f), and also some of the enclaves includes olivine ± clinopyroxene crystal clots, plagioclase glomerocrysts and quartz xenocrysts with ocelli (Gençoğlu Korkmaz et al. 2021, 2022).

Investigated volcanic rocks have low LOI (loss on ignition) values (< 2 wt. %), indicating that the effect of alteration is minor. The Karapınar volcanic rocks (KB1, KB2, and MME) exhibit basalt, basaltic–andesite composition in the total alkali-silica rock classification diagram (Fig. S3; Le Bas et al. 1986). However, in Zr/Ti versus Nb/Y classification diagram (Pearce 1996), studied rocks were dominantly plotted as basaltic–andesite and basalt, and rarely plotted into the alkali basalt field (Fig. S3). The KB1 rocks have a transitional (calc-alkaline–mildly alkaline) geochemical affinity, whereas KB2 rocks and their enclaves are calc-alkaline (Irvine and Baragar 1971) in composition.

4.2. Whole-rock chemistry

The SiO_2 versus major and trace element variation diagrams (Fig. S4) for the studied rocks generally show linear trends with progressive differentiation from basaltic to intermediate rocks. The diagrams indicate two different volcanic suites and the MMEs plotting between the KB1 and KB2 group rocks. The SiO_2 vs. MgO and CaO plots show a negative trend following sharp MgO and CaO inflections (Figs S4a, S4b). The SiO_2 vs. K_2O and TiO_2 variations are characterized by linear decreases in KB1 and MME rocks. However, KB2 rocks display a flat trend or slight increases in SiO_2 vs. Ba, Sr, Ni, and Zr (Fig. S4).

In NMORB normalized diagrams (Hofmann 1988; Fig. S5), KB1 and KB2 basaltic rocks display similar enrichments in LILE (large ion lithophile elements) such as Rb, Sr, K, and troughs of some HFSE (high field strength elements) such as Ti, Ta, Nb, which suggests derivation from similar magma source(s). Chondrite-normalized REE (rare earth element) distributions (Nakamura 1974) show enrichments of LREE, relative to HREE (Fig. S5). All Karapınar basaltic rocks show slightly fractionated chondrite-normalized REE patterns with La_N/Lu_N = 6.9–13 and are parallel to each other, revealing a similar or the same source area for these volcanic rocks. Although they demonstrate similar orogenic type geochemical patterns in the NMORB normalized diagram, the studied basaltic rocks (KB1–KB2) are different, as detailed in the discussion section 5.

4.3. Olivine major and trace element chemistry

Fourteen olivine grains from KB1 (N = 3), KB2 (N = 5), and MME (N = 6) were analyzed by EPMA for the major oxides, and eight of them KB1 (N = 3), KB2 (N = 4), and MME (N = 1) were also analyzed for trace elements using LA–ICP–MS. The primitive olivines (Mg-rich) in KB1 group rocks show normal zoning with TiO_2, MgO, Mg #, forsterite ($Fo = 100 \times Mg/(Mg + Fe^{total})$), Ni-rich cores and they exhibit multiple (normal to inverse) zoning with Ca, Cr, Co, Sc, V, Mn, Li, and Zn (Tab. S2). The boundaries between the cores and the rims are visible in BSE images (Fig. S6). However, the olivines from KB2 and MME show both normal and reverse zoning with Ca, Cr, Co, Sc, V, Mn, Li, and Zn (Tab. S2). Olivine cores in all basalts have 1600–2600 ppm CaO and contain ~ 1000–1300 ppm Mn. Furthermore, they include Fo and Fe/Mn ranging from ~ 84 to 89 and from ~ 70 to 99, respectively. The Ni contents of the olivine (core = ~ 2300–3100 ppm; rim = ~ 810–1500 ppm) have a positive correlation with Fo (89–87) in the most primitive basalts (KB1). The KB2 olivines are richer in Ni (~ 1200–2500 ppm) relative to the KB1 olivines. The Ni/Co values (~ 23) of Mg-rich olivines (KB1 olivines) are higher than those of Fe-rich (KB2) olivines (~ 16). Moreover, the KB1 and KB2 olivine cores contain Li contents from 1.8 to 2.2 ppm and 1.5 to 1.6 ppm, respectively. Zinc concentrations of the olivines range from 75 to 242 ppm and exhibit a direct relationship with Mn/Zn value and Li, Mn contents (Tab. S2). The olivines from MME display progressive normal zoning with decreasing Ni (~ 1800–1200 ppm) and Fo (86–75) and increasing Mn, Li, and Zn (Mn = 1400–1900 ppm; Li = 2.5–10 ppm; Zn = 89–189 ppm) from the core to the rim. Zone boundaries between the cores and the rims of the MME olivines are sharp, indicating abrupt compositional variations.

4.4. Olivine stable isotope composition

The olivines from the Karapınar basaltic rocks (KB1, KB2, MME) have $\delta^{18}O$ ranging between 5.7 and 6.5 ‰

(Tab. S1). The $\delta^{18}O$ values of olivines from the enclaves (6.2 ‰) are much higher than those from their hosts (5.7 ‰). However, it is noteworthy that the olivines (5.7–6.4 ‰) from calc-alkaline basaltic rocks (KB2) yield lower $\delta^{18}O$ isotopic values than the olivines (6.5 ‰) from mildly-alkaline basaltic rocks (KB1).

5. Discussion

5.1. Petrogenesis and evolution of the Karapınar basaltic rocks

Major and trace element variations (Fig. S4) and REE patterns (Fig. S5) suggest that fractional crystallization (FC) processes played a significant role in the evolution of the Karapınar basaltic rocks. In particular, SiO_2 versus CaO and MgO depletions indicate the importance of the olivine and clinopyroxene fractionation in the formation of the rocks. Different trends in the Harker variation diagrams of the KB1 and KB2 units indicate that they have different magmatic histories. Based on whole-rock major (i.e., high SiO_2, K_2O) and trace elements (i.e., high Rb, Ba, K, U, Pb, Th, Ce), we suggest that the parental melts to the KB2 rocks undergone more significant crustal contamination relative to the KB1 ones. Along with that, based on Nb/Ta and Nb/U ratios, the effect of crustal contamination on the composition of ne-normative alkali basalts (KB1) is insignificant during the magma ascent through the continental crust relative to the calc-alkaline basalts (KB2) as also shown by Gençoğlu Korkmaz et al. (2022). This assumption is further supported by the petrographic signatures, such as the presence of ocelli and embayed-quartz, sieved-plagioclase, biotite, and amphibole xenocrysts presented in KB2 rocks. The linear trends on Harker diagrams suggest that the magma mixing process may have played a key role in the evolution of the enclaves. The linear extension of the MME between KB1 and KB2 in all variation diagrams suggests that they were formed by the mixture of these two basaltic groups. To evaluate the possible magma mixing process, we performed a mixing calculation by using major elements of the most primitive (KB1/GK-31) and the most evolved (KB2/KR-30) end-members in the Igpet software (version 2014 of Carr 1990). Based on this modeling, the composition of the MME can be best explained by mixing the mildly alkaline and calc-alkaline volcanic units. The MME has $\sum r^2$ values ranging from 0.75 to 0.81. However, the $\sum r^2$ should be <0.2; therefore, the acceptable solution's higher values may be explained by differentiation after mixing processes (Mann 2010). The best solution indicates a mixing of ~62 % KB1 (GK31) and ~38 % KB2 (KR30) to reproduce a hybrid MME (Tab. S1).

Except for some of the olivine grains from the KB2 and MME suites, olivine grains are generally in equilibrium with their host liquid ($Kd_{Fe-Mg} = 0.30 \pm 0.03$; Tab. S2). The olivine phenocrysts from the KB1 basalts have high Fo values up to 89 in their cores, similar to mantle peridotite (Best 2003), and show normal zoning. However, high Fo values are not always considered to be the hallmark of mantle peridotite olivine. For example, experimental studies suggest that even minerals with very high Mg# may crystallize directly from basaltic magmas (Gaetani and Grove 1993; Feig et al. 2006; Koepke et al. 2009). Increased oxygen fugacity will decrease the Fe^{2+}/Fe^{3+} value of the melt, increasing the Fo content of olivine (Feig et al. 2006, 2010). Furthermore, studied olivine phenocrysts contain up to ~800 ppm Al while 80 % of mantle olivines have less than 130 ppm Al (De Hoog et al. 2010; Foley et al. 2013). The $\delta^{18}O$ values of the Karapınar olivines (+5.7–6.5 ‰) are higher than those reported for MORB (+5.1–5.4 ‰) and close to OIB-EMII (+5.4–6.1 ‰) (Eiler et al. 1997). It is well-known that one of the most reliable criteria for distinguishing between xenocryst (mantle olivine) and phenocryst is the CaO content of olivine. In this respect, olivine phenocrysts generally have a higher CaO content (CaO >0.1 wt. %) than mantle peridotite olivine (Thompson and Gibson 2000; Ying et al. 2010; Wang et al. 2011). Considering all this information, we interpret the Karapınar olivines as phenocrysts crystallized from the parental magma due to their high CaO (0.15–0.22 wt. %) and Al (195–390 ppm) contents as well as $\delta^{18}O$ values. Furthermore, the fact that the olivines of the calc-alkaline basaltic rocks (KB2) yield lower $\delta^{18}O$ values than the olivines of the mildly alkaline basaltic rocks (KB1) may be associated with the changing in the water content of the magma and/or the incorporation of different materials during suggested crustal contamination (Dobosi et al. 1998; Downes 2001; Gertisser and Keller 2003).

The investigated olivine have variable zoning (normal, inverse, oscillatory) in terms of Ca, Co, Cr, Mg, Fe, Sc, V, Ni, and Mn contents (Tab. S2). These chemical variations most likely reflect magma recharge or mixing processes in the magma chamber (Humphreys et al. 2006; Stroncik et al. 2009; Hu et al. 2018; Jankovics et al. 2019). The presence of magmatic enclaves, olivine ± clinopyroxene crystal clots, plagioclase glomerocrysts, embayed and ocelli quartz xenocrysts in the Karapınar basalts may be critical evidence for the existence of recharging (magma mixing) and reheating events with convection in a magma chamber (Figs. 2, S6; Jankovics et al. 2019). Furthermore, the KB1 group rocks include two olivine crystals having quite different Ni (~2300–3100 ppm), Fo (87–89) contents, and Mn/Zn (15–13), Ni/Co (19–23) values in their cores (Tab. S2), which is indicative for recharging processes (Nakagawa et al. 2002). Thus, we suggest

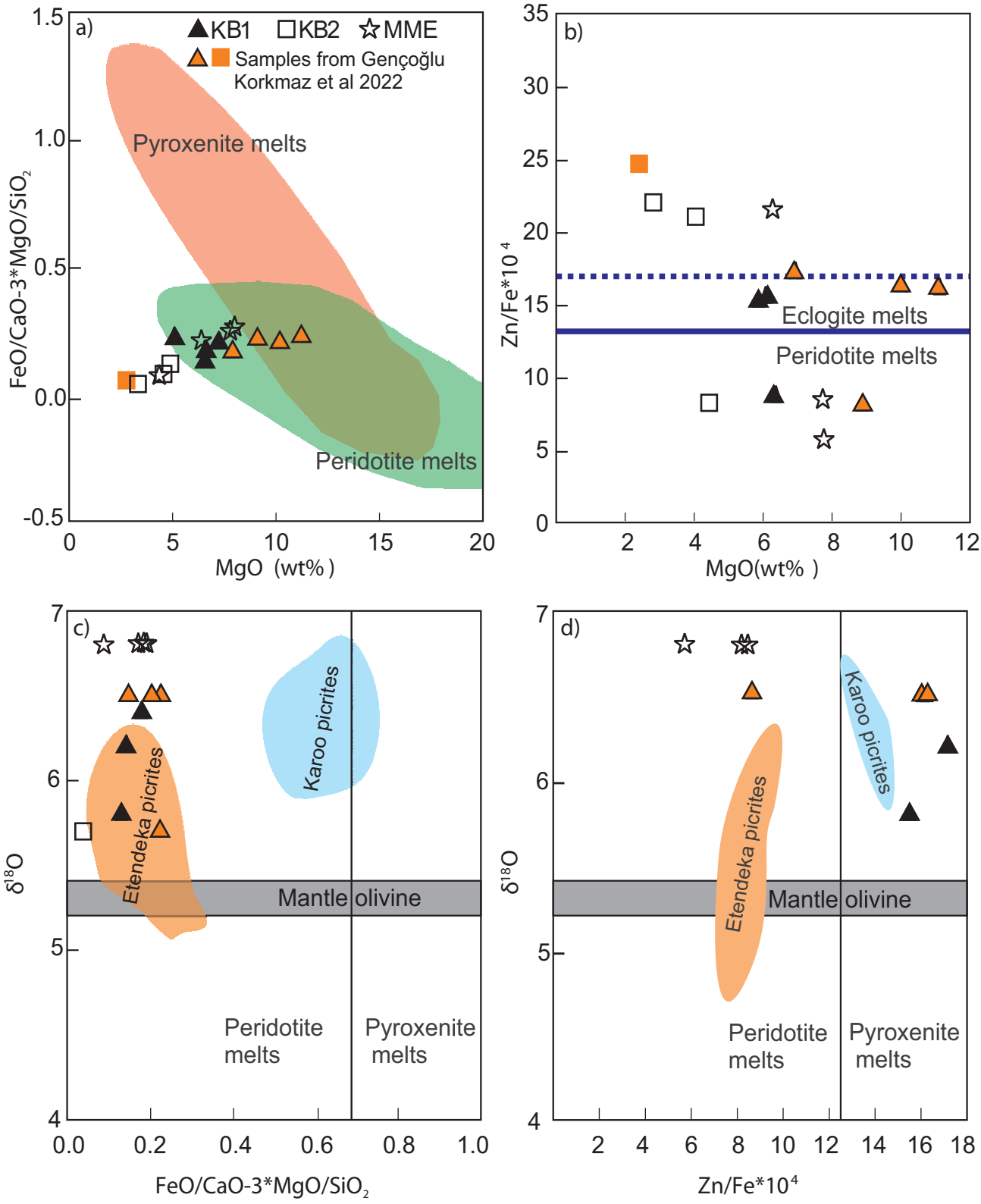

Fig. 3. (a) FC3MS (FeO/CaO-3*MgO/SiO2, all in wt. %) vs. MgO wt. % plot (Sheldrick et al. 2018), (b) Zn/Fe (× 10^4) values vs. MgO wt. % plot, (c) $\delta^{18}O$ (‰) vs. FC3MS and (d) $\delta^{18}O$ (‰) vs. Zn/Fe (× 10^4) diagrams of the Karapınar basalts. $\delta^{18}O$, FC3MS, and Zn/Fe (× 10^4) ratios for Karoo and Etendeka olivines (in southern Africa) are from Howarth and Harris (2017). The $\delta^{18}O$ value of mantle olivine is from Chazot et al. (1997). The upper eclogite and the peridotite melts fields are from Chazot et al. (1997).

that ascending primitive magma plucked these olivines, glomerocrysts, and the crystal clots from different parts of the magma chamber (the wall or the basement) during replenishment processes and carried them to shallower levels. Furthermore, plagioclase phenocrysts with abundant sieve textures in the basalts may be evidence of decompression or reheating events in the magma chamber (Kurt et al. 2019; Gençoğlu Korkmaz and Kurt 2021). Along with them, olivine with skeletal textures (Fig. S6) may be evidence for rapid (under) cooling (Lofgren 1974). To summarize, based on the mineralogical and textural properties of the rocks and the chemical composition of the olivines, we suggest that recharging events and also the decompression process may play a significant role in the evolution of the Karapınar basaltic rocks.

5.2. Insights from primitive basalts

The composition of mafic rocks (MgO > 4 wt. %; Peccerillo 2005) gives the most accurate knowledge regarding mantle source compositions because they have the closest composition to primary melts derived from the upper mantle. Basalts with 1000 ppm Cr, 400 ppm Ni, 8 wt. % MgO (Best 2003), and low LILE/HFSE values (Weaver 1991) indicate derivation from a primary mantle source. The studied mildly alkaline basalts (GK31 and L8) are characterized by an almost primitive chemical signature with their Ni (186–221 ppm), Cr (383–540 ppm) and MgO (10–11.12 wt. %) contents (Tab. S1). Accordingly, it is recommended that these rocks may be the right guide for the interpretation and the determination of the mantle source characteristics, as they would give more accurate fingerprints regarding the mantle source. Low HREE concentrations (Yb < 2 ppm) and Y (< 25 ppm) contents and fractionated HREE patterns ($Dy/Yb_N > 1$) in KB1 basalts may indicate residual garnet in the source of the rocks (Tab. S1 and Fig. S5; Kheirkhah et al. 2015). An excess of clinopyroxene in the residual source decreases the Zr and Hf contents of the forming melts and leads to negative Hf and Zr anomalies. Moreover, clinopyroxene ($D_{Zr/Hf} < 1$) may control the Zr/Hf fractionation (Li et al. 2015). Investigated basalts have higher Zr/Hf ratios (average 39) than primitive mantle (Zr/Hf = 34–36). So, the slightly negative Zr anomalies (Fig. S5a), and moderately high Zr/Hf ratios (Tab. S1) in the Karapınar basalts might indicate a Cpx-rich residue in the source as in Zhejiang basalts which were derived from a heterogeneous mantle source produced by mixing of pyroxenitic and peridotitic sources (Li et al. 2015). Along with that, Karapınar basalts are characterized by moderately high La/Yb (11.40–13.67), Fe/Mn (54–65), and Nb/Ta (14.83–19.20) ratios, which could be used as a major fingerprint for the presence of residual clinopyroxene, garnet and rutile in the mantle source (Li et al. 2015). The crystallization temperatures for the Karapınar basalts can be estimated using the clinopyroxene–liquid and olivine–liquid thermobarometers (Putirka 2008). Clinopyroxene and olivine compositions that fall well within the Fe–Mg equilibrium fields are used, and the bulk-rock compositions are considered as liquid compositions. Kurt et al. (2019) reported that clinopyroxene–liquid thermobarometry indicates clinopyroxene crystallization temperatures ranging between 1173–1251 °C. Moreover, in this study, we propose that olivines' calculated crystallization temperatures range from 1210 to 1250 °C (Tab. S2). These temperatures are almost close to the assumed temperature at the base of the sub-continental lithospheric mantle (SCLM) beneath Central Anatolia and also resemble the potential mantle temperature (1280–1400 °C; Herzberg et al. 2007) of the depleted asthenosphere mantle as in Halaqiaola basalts (Chinese Altai, central Asia; Zhang et al. 2019). These were continental OIB-like basalts and stemmed from a hybrid source containing pyroxenite and peridotite components. Along with that, some recent studies (McNab et al. 2018; Kürkcüoglu and Yürür 2022) suggest a new model regarding the source of the young basalts from the northernmost end of the Cappadocian region in Central Anatolia. McNab et al. (2018) report that the mantle underlying Central Anatolia was quite hot with a composition similar to that of OIB source reservoirs; thus, magmas presumably stemmed from the asthenosphere. Moreover, Kürkcüoglu and Yürür (2022) claimed that young basalts from the CVP could be derived from a marble-cake-type peridotite–pyroxenite mixed source. However, previous studies claimed that the basalts from the southwestern part of the CVP were derived from subduction-modified mantle peridotite (Reid et al. 2017; Uslular and Gençalioğlu-Kuşcu 2019). Also, the recent studies evaluated and used the whole-rock FC3MS ($FeO^T/(CaO^{-3} \times MgO/SiO_2)$, all in wt. %) parameter, which was produced by Yang and Zhou (2013) to determine the source lithology of the rocks. The partial melting products of a pyroxenitic source contain high FC3MS values (> 0.65; Yang and Zhou 2013) and commonly have lower CaO contents than peridotitic sources (Herzberg Herzberg; Zhang et al. 2012; Søager et al. 2015). Although the investigated basalts have FC3MS values below 0.65 (Fig. 3a), they have a narrow range of MgO and lower CaO contents consistent with a pyroxenite source. Furthermore, Zn/Fe is a possible tracer for mantle heterogeneities because it is susceptible to the existence of clinopyroxene and garnet-rich lithologies (Le Roux et al. 2010). The peridotitic partial melts have lower Zn/Fe (× 10000) values (typically 8–10), whereas a pyroxenite can generate melts with higher Zn/Fe (× 10000) values (> 14; Le Roux et al. 2010). The most primitive basalts (KB1; MgO ~ 10–12 wt. %) contain Zn/Fe (× 10000) values (~ 16) similar to those of pyroxenite-derived melts.

Considering their MgO contents and FC3MS values, Zn/Fe values of the Karapınar basalts indicate that lavas may be descended from the mixing of peridotitic and pyroxenitic melts (Figs 3b–3d; Guo et al. 2015; Sheldrick et al. 2018). Moreover, the $\delta^{18}O$ values of the KB1 olivines (~6.5 ‰) and whole-rock Zn/Fe (× 10000) values (~16) of the KB1 are similar to basaltic rocks derived from pyroxenitic melts, like Karoo picrites from southern Africa (Howarth and Harris 2017; Figs 3c, 3d). Combined with whole-rock geochemistry and $\delta^{18}O$ values of olivine, we suggest that Karapınar mafic volcanism has asthenospheric source fingerprints, and the KB1 rocks are also likely to have formed from a heterogeneous source consisting of peridotite plus metasomatic pyroxenite produced by the interaction of silica-rich melts derived from subducting oceanic crust with the surrounding peridotite which included recycled oceanic crustal material (Harris et al. 2015; Howarth and Harris 2017; Kamenetsky et al. 2017).

5.3. Olivine trace element characteristics to decipher the source lithology

Olivine from the most primitive basalts can give accurate information about the source lithology. Recent studies on olivine trace element contents from the large igneous province (LIP) and ocean island (OIB) basalts clearly aimed to interpret and detect mantle source lithology. These studies demonstrate that many LIP and OIB magmas have signatures that can be attributed to melts derived from pyroxenite in their sources (Sobolev et al. 2005, 2007; Gurenko et al. 2010; Barker et al. 2014; Søager et al. 2015; Howarth and Harris 2017). For example, Mn/Fe ratios and Ni contents of olivine phenocrysts have been used to detect the mineral composition of the mantle source of the host magma. However, high Ni and low Mn/Fe ratios are likely to be signatures of the high temperatures and pressures of melting and probably high water contents in some peridotitic mantle sources (De Hoog et al. 2010). Moreover, Gleeson and Gibson (2019) suggest that mafic magma recharge from the oceanic crust may cause the enrichment of Ni in olivine in basalts. However, that process is ruled out due to the geological setting for those continental intra-plate basalts, as in the eastern Australia basalts (C-OIB; thick >70 km lithosphere; Liu et al. 2021). Hence, the other mantle source lithology indicators such as Li, Zn, Ca, Al contents, Ni/Co, Fe/Mn, Mn/Zn, Zn/Fe ratios of the olivine grains should also be used to provide constraints on the mantle source of the basaltic magmas (De Hoog et al. 2010; Guo et al. 2015; Søager et al. 2015; Howarth and Harris 2017; Howarth and Udry 2017). Lithium and Zn contents of olivine are distinctive for identifying continental crustal recycling in the source of the rocks (Foley et al. 2013) and may serve as a tracer of pyroxenite in the source. Olivine cores from KB1 and KB2 contain Li 1.5–2.2 ppm (Tab. S2), similar to those in basalts from ocean islands (Jeffcoate et al. 2007; Chan et al. 2009; Foley et al. 2013). Zn contents of the same olivines positively correlate with Li and range from 79 to 105 ppm in the cores. Lithium and Zn enriched rims of the studied

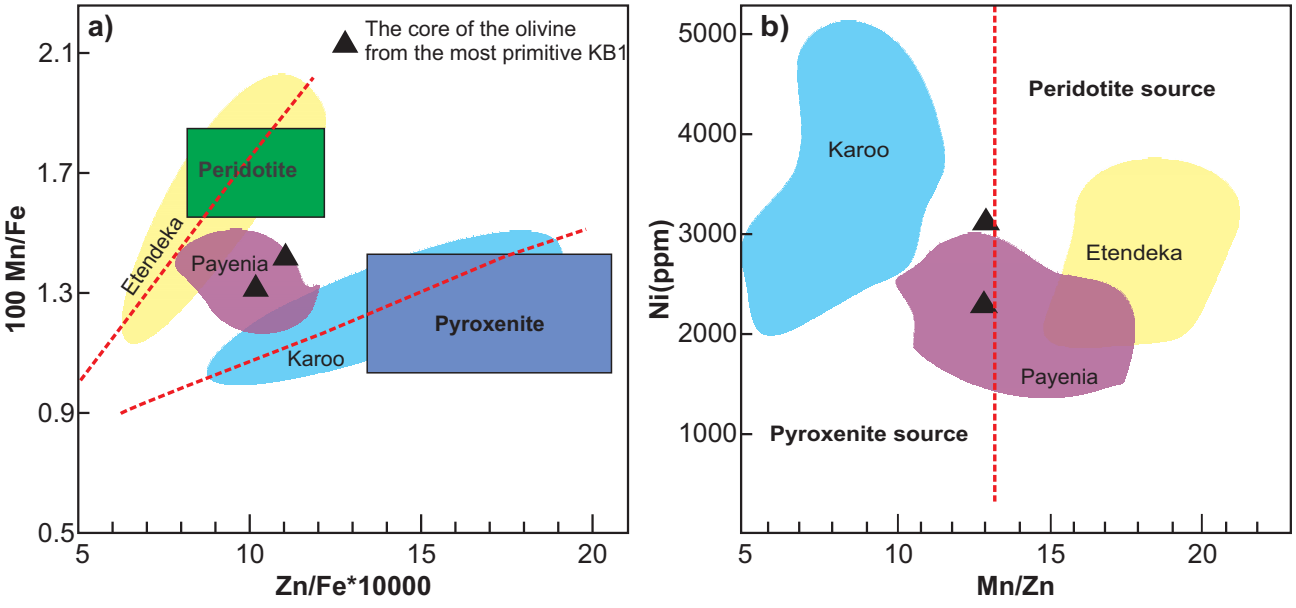

Fig. 4. Selected trace element variations of olivine from the Karapınar basalts, and comparison with different olivines in the literature. (a) 10000 Zn/Fe vs. 100 Mn/Fe diagram is modified from Sobolev et al. (2007) and Le Roux et al. (2010), and (b) Ni (ppm) vs. Mn/Zn ratio plot for the most primitive olivine cores, The Payenia olivines (Argentina) which originated from mixed peridotite–pyroxenite mantle sources are from Søager et al. (2015). The Karoo olivines which descend from pyroxenitic sources and Etendeka olivines which are derived from peridotitic sources are from Howarth and Udry (2017).

olivine indicate the source containing recycled continental crust (Foley et al. 2013), as in Hawaiian olivines having low Li (1.1–2.1 ppm) and variable Zn in their cores (Neumann et al. 1999). Some of the experimental studies suggest that higher Zn/Fe, Fe/Mn, Co, Fe, Ni, Mn, Zn, as well as lower Mn/Fe, Ni/Co, Mn/Zn, Co/Fe of the olivine support the evidence for pyroxenitic melts rather than peridotitic melts in the source (Sobolev et al. 2007; Le Roux et al. 2010; Herzberg 2011; Le Roux et al. 2011; Søager et al. 2015). The investigated olivines are Ni-rich (>2000 ppm), Ca-poor (<1600 ppm), and contain low 100×Mn/Fe (<1.4). The olivine cores of the most primitive basalts (KB1; MgO >10 wt. %), Fe/Mn (71–76), Ni (2300–3100 ppm), Co (128–142 ppm) contents and high Ni/Co (~24) values resemble those of pyroxenitic (Ni/Co >20; Foley et al. 2013) sources (Sobolev et al. 2007; Le Roux et al. 2010; Herzberg 2011; Le Roux et al. 2011; Søager et al. 2015). Also, Zn/Fe ratios of the olivine phenocrysts have been utilized in many studies to distinguish pyroxenitic and peridotitic melts from each other. As Zn/Fe (×10000) values of the peridotitic olivines generally range from 9.3–10 (Le Roux et al. 2010) and olivine in equilibrium with experimental pyroxenite melts have Zn/Fe (×10000)>14 (Le Roux et al. 2010, 2011; Zhang et al. 2012), the most primitive olivine from KB1 probably originated from a pyroxenite dominated source due to their higher Zn/Fe (×10000) values (10–11; Fig. 4a). Furthermore, Mn/Zn values of the olivine can be a practical discriminator for source lithology (Howarth and Harris 2017). Whereas olivine derived from pyroxene-dominated sources contain low Mn/Zn (<13), olivine generated from peridotitic partial melts has a high Mn/Zn (>15) ratio (Howarth and Harris 2017). The olivine cores from the KB1 contain Mn/Zn ranging from 12–15, indicting pyroxenite dominant sources (Howarth and Harris 2017; Fig. 4b). Hence, the Karapınar basalts have characteristics of a heterogeneous source derived from the mixing of pyroxenite and peridotite melts based on Zn/Fe, Mn/Fe, and Ni contents, similar to the Payenia basalts from Argentina (Søager et al. 2015; Fig. 4). Moreover, forsterite content versus Ca, Ni, Fe/Mn, and 100×Mn/Fe diagrams also indicate that most sampled olivines lie between the two source areas suggesting mixing of melts derived from pyroxenitic and peridotitic sources-derived (Fig. 5; Sobolev et al. 2007; Guo et al. 2015; Søager et al. 2015; Howarth and Harris 2017; Liu et al. 2021).

Estimation of the proportion of pyroxenite source components in the mantle source could be carried out using the equations (eq.1 and 2) derived by Sobolev et al. (2007);

$$Xpx = 3.48 - 2.071 \times (100 \times Mn/Fe) \quad (1)$$

$$Xcrc = Xe / Fe\left[\frac{(1-Xpx)}{Xpx} \times \left(Fpx\frac{1}{Fpe}\right) + \frac{1-Fe}{Fe} \times Xe + 1\right] \quad (2)$$

Xe = Proportion of eclogitic melts required to generate hybrid pyroxenite from peridotite, *Xpx* = Proportion of pyroxenitic melts, *Xcrc* = Amount of recycled oceanic crust, , *Fe* = The melting degree of eclogite, *Fpx* = The melting degree of pyroxenite, *Fpe* = The melting degree of peridotite.

Sobolev et al. (2007) used olivine phenocryst composition to detect the proportion of the pyroxenitic lithology involvement in komatiites (20 to 30 % pyroxenite), ocean islands and continental basalts (many of them >60 % pyroxenite), and mid-ocean ridge basalts (10 to 30 % pyroxenite). Due to the heterogeneous lithospheric thickness in the Central Anatolia, within plate magmas WPM-thick (lithosphere >70 km; Hawaii-OIB) setting standard values (Xe = 50 %, Fpe = 10 %, Fpx = 50 %, Fe = 50 %) and WPB-thin (lithosphere <70 km; C-OIB) setting standard values (Xe = 50 %, Fpe = 20 %, Fpx = 50 %, Fe = 50 %; Sobolev et al. 2007) were utilized to evaluate the proportions of the peridotite and pyroxenite in the mantle sources for the most primitive samples (KB1; MgO >10 wt. %; Tab. 1). Following these assumptions, for the olivine phenocryst from the most primitive samples (KB1), we calculated the same Xpx and Xpe proportions with an average of ~70 % and 30 %, respectively. However, it is observed that the proportion of the recycled eclogitic material Xcrc is changed with the lithospheric thickness

Table 1 The proportions of the recycled eclogite (Xcrc), peridotite (Xpe), and pyroxenite (Xpx), in the source of the most primitive basalts (KB1).

Sample/Circle/Spot (c)ore/(m)id/(r)im		Proportions of the melts in the heterogeneous source			Average proportions (%)		
		Xpx	Xcrc (WPM--THICK or THIN)	Xpe (1–Xpx)	Xpx	Xcrc (WPM--THICK or THIN)	Xpe
KB1	GK-31-C1-1m	0.60	0.20	0.40	69.54	28.57	30.46
	GK-31-C3-1m	0.70	0.28	0.30			
	GK-31-C3-1c	0.55	0.18	0.45			
	GK-31-C6-1m	0.87	0.44	0.13			
	GK-31-C6-1c	0.76	0.33	0.24			

$Xpx = 3.48 - 2.071 \times (100 \times Mn/Fe)$

$Xcrc = Xe/Fe\left[\frac{(1-Xpx)}{Xpx} \times \left(Fpx\frac{1}{Fpe}\right) + \frac{1-Fe}{Fe} \times Xe + 1\right]$ (Sobolev et al. 2007)

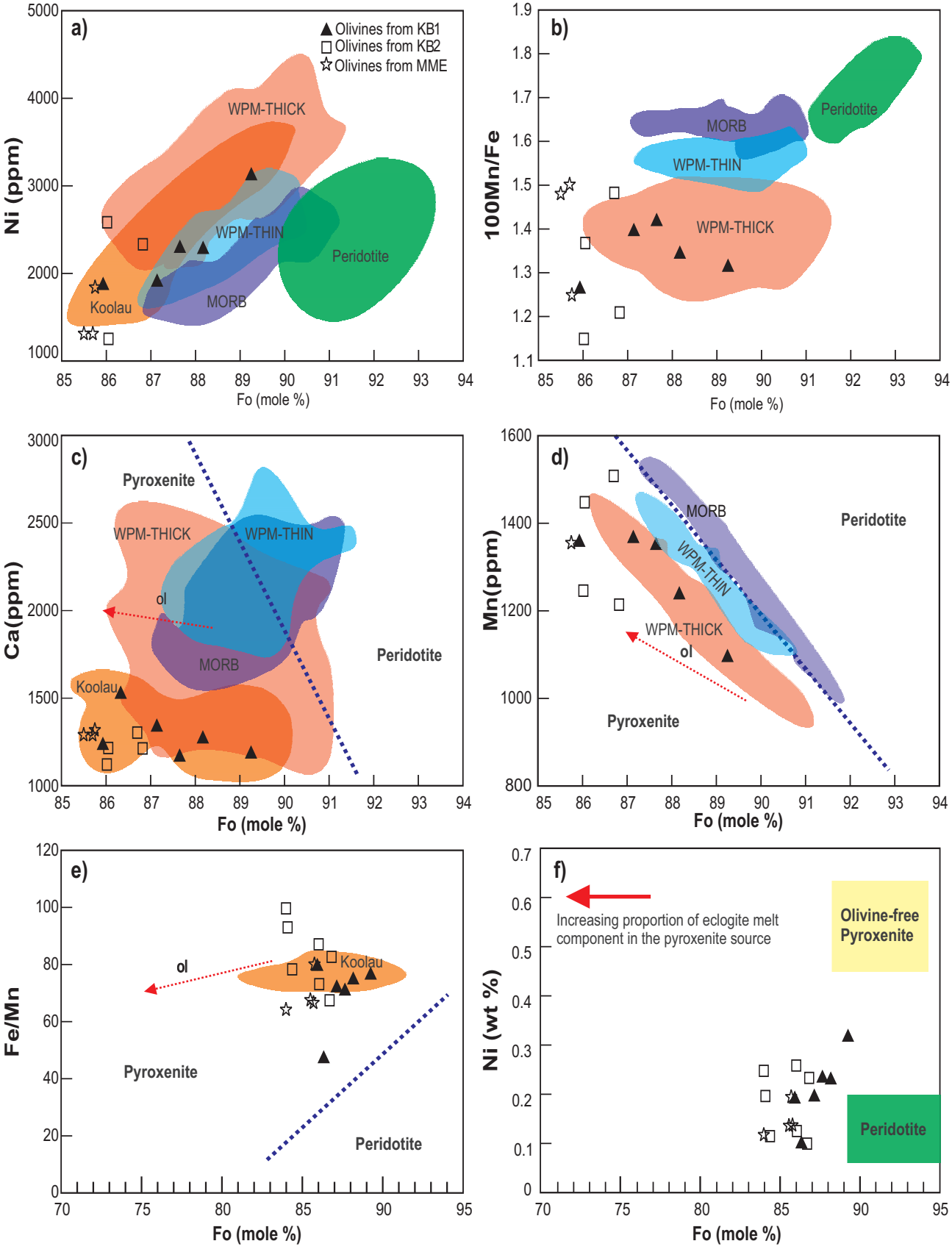
a)
Olivines from KB1
Olivines from KB2
Olivines from MME
WPM-THICK
WPM-THIN
Peridotite
MORB
Koolau
Ni (ppm)
Fo (mole %)
b)
Peridotite
MORB
WPM-THIN
WPM-THICK
100Mn/Fe
Fo (mole %)
c)
Pyroxenite
WPM-THICK
WPM-THIN
ol
MORB
Peridotite
Koolau
Ca(ppm)
Fo (mole %)
d)
MORB
Peridotite
WPM-THIN
WPM-THICK
ol
Pyroxenite
Mn(ppm)
Fo (mole %)
e)
ol
Koolau
Pyroxenite
Peridotite
Fe/Mn
Fo (mole %)
f)
Increasing proportion of eclogite melt component in the pyroxenite source
Olivine-free Pyroxenite
Peridotite
Ni (wt %)
Fo (mole %)

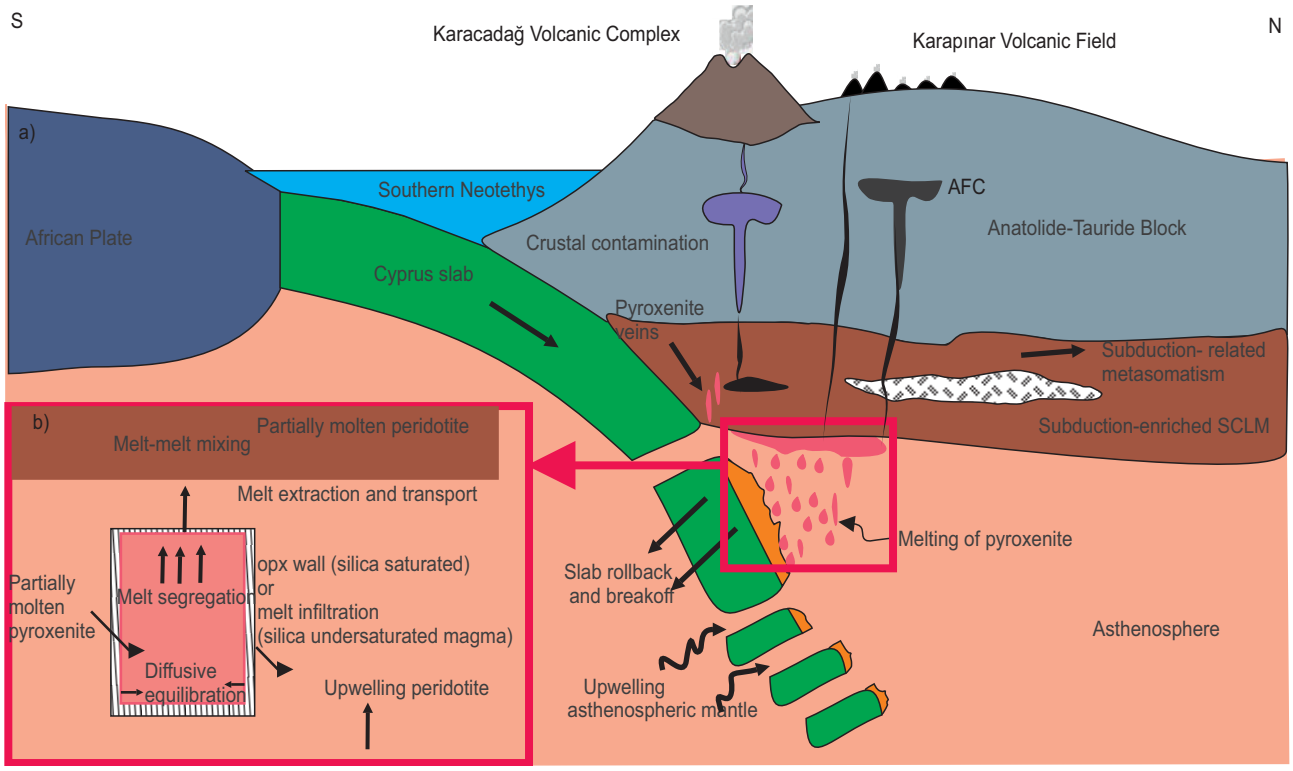

Fig. 6. An illustrative sketch showing the petrogenesis of the Karapınar rocks. Mixing of pyroxenite partial melt with peridotite partial melt. (a) A schematic tectonomagmatic model for the Neogene-Quaternary Karapınar-Karacadağ Volcanic Rocks. (b) A schematic model of partial melting processes of heterogeneous mantle modified from Kogiso et al. (2004b).

(thin <70 km lithosphere Xrc=~39 %, thick >70 km lithosphere; ~29 %; Tab. 1).

5.4. Petrogenetic model of the volcanic rocks from the southwest part of the CVP

Slab roll-back, retreat and slab tearing processes are critical in volcanism along Central Anatolia. During these processes, the melts stemmed from the asthenosphere interacting with the lithospheric mantle. Recent geophysical, geological and tectonic studies show that the Cyprus subduction zone has been in a slab roll-back phase and actively retreating relative to Central Anatolia from the Middle Miocene onwards (Fig. 6a; Faccenna et al. 2006; van Hinsbergen et al. 2010; Biryol et al. 2011; Schleiffarth et al. 2018; Reid et al. 2019).

During subduction, recycled oceanic crust is subjected to a complicated physicochemical evolution, melts and converts into silica-undersaturated or silica-saturated pyroxenite (Kogiso et al. 2004b).The boundaries of the mantle pyroxenite interact continuously with mantle peridotite and they are impacted by diffusion due to physicochemical differences between pyroxenite and peridotite (Fig. 6b). During partial melting, an internal separation process (Kogiso et al. 2004a, b) or infiltration into the peridotite (Daines and Kohlstedt 1993; Kogiso et al. 2004b) gives rise to melt separation from the residual pyroxenite. The reaction and stabilization of the melt with the surrounding mantle produces a heterogeneous mantle source.

Based on the olivine trace and major element concentrations, we suggest that the post-collisional mafic magmas in the Konya-Karapınar region were derived from a hybrid peridotite-pyroxenite mantle source that has a direct relationship to the subduction processes (Fig. 6). Mixing of varied proportions of melts derived from pyroxenitic and peridotitic sources produced the most

⇦

Fig. 5. Diagrams showing selected trace element distributions of olivine phenocrysts from the Karapınar basalts and peridotite-pyroxenite melt areas (after Herzberg (2011). (a) Ni (ppm) vs Fo (mol. %); (b) 100 Mn/Fe *vs.* Fo (mol. %); (c) Ca (ppm) *vs.* Fo (mol. %); (d) Mn (ppm) *vs.* Fo (mol. %); (e) Fe (ppm)/Mn (ppm) *vs.* Fo (mol. %); (f) Ni (wt. %) *vs.* Fo (mol. %) variation diagrams of olivine phenocrysts %. Green ellipse represents the field of olivine compositions from a peridotitic source (Sobolev et al. 2007). The tectonic areas that include MORB, WPM-THIN (thin lithosphere < 70 km), OIB and LIP WPM-THICK (thick lithosphere > 70 km) and Koolau olivines area are modified from Sobolev et al. (2007). Blue dashed lines are the discriminator lines for the fields of olivines that originated from pyroxenitic and peridotitic partial melts (Herzberg 2011). Red dashed lines display olivine fractional crystallization trend (Sobolev et al. 2007). (f) The red arrow depicts pyroxenitic sources comprising an increasing subducted crustal component, as well as olivine-free pyroxenite-derived and mantle peridotite-derived partial melts areas, are from Guo et al. (2015).

primitive mildly alkaline mafic magmas in the southwest part of the CVP.

6. Conclusions

Here, we amalgamated the EMP major and minor, and LA–ICP–MS trace element compositions, as well ^{18}O isotope values of the olivines with major and trace element whole-rock data to detect and confine the mantle source lithology of the Karapınar basalts. This study demonstrates that for the first time, olivine major-trace element data could serve as a powerful tool to unravel the genesis of the Quaternary-aged post-collisional mildly alkaline basaltic rocks in the CVP. Two geochemical types represent the Karapınar basalts; KB1 is transitional (mildly alkaline to calc-alkaline), high-MgO basalt (> 10 % MgO) with primitive olivine (Mg# of 88–89), and KB2 is calc-alkaline, evolved-contaminated basalt including lower Mg# of olivine. The study's main aim is to understand and evaluate the petrogenetic evolution of the Karapınar basalts, mainly focusing on the possible involvement of pyroxenitic melts in the source and their later evolution in the crustal levels. Therefore, KB1 group mildly alkaline basalts having high MgO (10–12 wt. %) content and primitive Nb/U (2–12) and Nb/Ta (17–19) ratios were used for the mantle source interpretations, while more evolved KB2 basaltic rock were utilized for the interpretation and the evaluation of the crustal processes.

Combined with the mineralogical and textural properties of the rocks, the chemical composition of the olivines reveals that recharging events and the decompression process could affect the evolution of the Karapınar basalts. KB1 basalts have lower CaO content and higher Zn/Fe ratios than basalts derived from the peridotitic source. The most primitive olivine phenocrysts from these basalts include high Ni content, Ni/Co, Zn/Fe, Fe/Mn ratios, and low Mn/Zn ratio relative to those from basaltic rocks derived from the peridotitic source. Hence these data reveal that KB1 basalts from the southwestern part of the CVP originated from a heterogeneous mantle source consisting of at least two lithologies (e.g., peridotite and pyroxenite). We recommend that the heterogeneous source be produced by mixing metasomatized peridotitic and pyroxene-rich mantle being present beneath the Anatolia.

Based on the calculations (WPM-thin; < 70 km and WPM-thick > 70 km), we propose a mixing model where the KB1 basalts were derived from a source containing ~ 70 % and 30 % of pyroxenite and peridotite, respectively. The pyroxenitic source has likely been generated by the interaction between the subducted oceanic crust-derived melts and the surrounding peridotite. The possible triggering mechanism for the melting of such a mixed source was the asthenospheric upwelling related to the roll-back and break-off of the Cyprus slab, from the middle Miocene onwards in the convergent system of the Afro–Arabian and Eurasian plates.

Acknowledgments This study was financially supported by Tubitak Caydag project number 118Y252 and Selcuk University Bap project number 17401117. We thank Professor Yusuf Kağan Kadioğlu, Dr. Kıymet Deniz, and Yebim for preparing the samples and realizing XRF and EPM analyses. The authors are deeply grateful to the handling editor Dr. Filip Tomek, and Assoc. Prof. Fatih Karaoğlan, as well as Assoc. Prof. Lukáš Ackerman for their critical and constructive comments that improved the quality of this paper. We are thankful to Dr. Gönenç Göçmengil for his valuable comments.

Electronic supplementary material. Supplementary material, consisting of supplementary figures S1–S4 and supplementary tables S5–S6, is available online on the Journal website (*http://dx.doi.org/10.3190/jgeosci.362*).

References

Artemieva IM, Shulgin A (2019) Geodynamics of Anatolia: lithosphere thermal structure and thickness. Tectonics 38: 4465–4487

Asan K, Kurt H, Gündüz M, Gençoğlu Korkmaz G, Morgan G (2021) Geology, geochronology, and geochemistry of the Miocene Sulutas volcanic complex, Konya-Central Anatolia: genesis of orogenic and anorogenic rock associations in an extensional geodynamic setting. Int Geol Rev 63: 161–192

Aydar E, Gündoğdu N, Bayhan H, Gourgaud A (1994) Volcanic-structural and Petrological Investigation of the Quaternary Volcanism of the Cappadocia Region. Turkish J Earth Sci 3: 25–42

Aydin F, Schmitt AK, Siebel W, Sönmez M, Ersoy Y, Lermi A, Dirik K, Duncan R (2014) Quaternary bimodal volcanism in the Niğde Volcanic Complex (Cappadocia, central Anatolia, Turkey): age, petrogenesis and geodynamic implications: Contrib Mineral Petrol 168: 1–24

Barker AK, Holm PM, Troll VR (2014) The role of eclogite in the mantle heterogeneity at Cape Verde. Contrib Mineral Petrol 168: 1–15

Bartol J, Govers R (2014) A single cause for uplift of the Central and Eastern Anatolian plateau? Tectonophysics 637: 116–136

Best MG (2003) Igneous and metamorphic petrology, 2nd ed. Wiley-Blackwell, pp 1–735

Biryol CB, Beck SL, Zandt G, Özacar AA (2011) Segmented African lithosphere beneath the Anatolian region inferred from teleseismic P-wave tomography. Geophys J Int 184: 1037–1057

Boschi L, Faccenna C, Becker TW (2010) Mantle structure and dynamic topography in the Mediterranean Basin. Geophys Res Lett 37: L20303, DOI:10.1029/2010GL045001

Carr M (1990) IGPET 3.0: Unpublished manual. Terra Sofia, Somerset, New Jersey, 46

Chan LH, Lassiter JC, Hauri EH, Hart SR, Blusztajn J (2009) Lithium isotope systematics of lavas from the Cook–Austral Islands: Constraints on the origin of HIMU mantle. Earth Planet Sci Lett 277: 433–442

Chazot G, Lowry D, Menzies M, Mattey D (1997) Oxygen isotopic composition of hydrous and anhydrous mantle peridotites. Geochim Cosmochim Acta 61: 161–169

Daines M, Kohlstedt DL (1993) A laboratory study of melt migration. Philos Trans Roy Soc, Series A: Phys Engineering Sci 342: 43–52

Dai LQ, Zheng F, Zhao ZF, Zheng YF (2018) Geochemical insights into the lithology of mantle sources for Cenozoic alkali basalts in West Qinling, China. Lithos 302–303: 86–98

De Hoog JCM, Gall L, Cornell DH (2010) Trace-element geochemistry of mantle olivine and application to mantle petrogenesis and geothermobarometry. Chem Geol 270: 196–215

Deniel C, Aydar E, Gourgaud A (1998) The Hasan Dagi stratovolcano (Central Anatolia, Turkey): evolution from calc-alkaline to alkaline magmatism in a collision zone. J Volcanol Geotherm Res 87: 275–302

Deniz K, Kadioğlu YK (2019) Investigation of feldspar raw material potential of alkali feldspar granites and alkali feldspar syenites within Central Anatolia. Bull Miner Res Explor 158: 265–289

Di Giuseppe P, Agostini S, Manetti P, Savaşçin MY, Conticelli S (2018) Sub-lithospheric origin of Na-alkaline and calc-alkaline magmas in a post-collisional tectonic regime: Sr–Nd–Pb isotopes in recent monogenetic volcanism of Cappadocia, Central Turkey. Lithos 316–317: 304–322

Dobosi G, Downes H, Mattey D, Embey Isztin A (1998) Oxygen isotope ratios of phenocrysts from alkali basalts of the Pannonian basin: Evidence for an O-isotopically homogeneous upper mantle beneath a subduction-influenced area. Lithos 42: 213–223

Dogan Kulahci GD, Temel A, Gourgaud A, Varol E, Guillou H, Deniel C (2018) Contemporaneous alkaline and calc-alkaline series in Central Anatolia (Turkey): Spatio-temporal evolution of a post-collisional Quaternary basaltic volcanism. J Volcanol Geotherm Res 356: 56–74

Downes H (2001) Formation and modification of the shallow sub-continental lithospheric mantle: a review of geochemical evidence from ultramafic xenolith suites and tectonically emplaced ultramafic massifs of western and central Europe. J Petrol 42: 233–250

Eiler JM, Farley KA, Valley JW, Hauri E, Craig H, Hart SR, Stolper EM (1997) Oxygen isotope variations in ocean island basalt phenocrysts. Geochim Cosmochim Acta 61: 2281–2293

Ercan T (1987) Orta Anadolu'daki Senozoyik Volkanizmasi. Bull Miner Res Explor 107: 119–140 (in Turkish)

Ercan T, Fujitami T, Matsuda J, Tokel S, Notsu K (1990) Hasandagı–Karacadag (Orta Anadolu) dolaylarındaki Senozoyik yaslı volkanizmanın kökeni ve evrimi. J Geomorph 18: 39–54 (in Turkish)

Faccenna C, Bellier O, Martinod J, Piromallo C, Regard V (2006) Slab detachment beneath eastern Anatolia: A possible cause for the formation of the North Anatolian fault. Earth Planet Sci Lett 242: 85–97

Faccenna C, Becker TW (2010) Shaping mobile belts by small-scale convection. Nature 465: 602–605

Feig S, Koepke J, Snow J (2006) Effect of water on tholeiitic basalt phase equilibria: An experimental study under oxidizing conditions. Contrib Mineral Petrol 152: 611–638.

Feig S, Koepke J, Snow J (2010) Effect of oxygen fugacity and water on phase equilibria of a hydrous tholeiitic basalt. Contrib Mineral Petrol 160: 551–568

Foley SF, Prelevic D, Rehfeldt T, Jacob DE (2013) Minor and trace elements in olivines as probes into early igneous and mantle melting processes. Earth Planet Sci Lett 363: 181–191

Gaetani G, Grove T (1993) The influence of water on the petrogenesis of subduction-related igneous rocks. Nature 365: 33–334

Gençalioğlu Kuşçu G, Geneli F (2010) Review of post-collisional volcanism in the Central Anatolian Volcanic Province (Turkey), with special reference to the Tepekoy Volcanic Complex. Int J Earth Sci 99: 593–621

Gençalioğlu Kuşcu G, Atilla C, Cas RAF, Kuşcu İ (2007) Base surge deposits, eruption history, and depositional processes of a wet phreatomagmatic volcano in Central Anatolia (Cora Maar). J Volcanol Geotherm Res 159: 198–209

Gençoğlu Korkmaz G, Kurt H (2021) Interpretation of the Magma Chamber Processes with the help of Textural Stratigraphy of the Plagioclases (Konya-Central Anatolia). European J Sci Tech 25: 222–237

Gençoğlu Korkmaz G, Asan K, Kurt H, Morgan G (2017) $^{40}Ar/^{39}Ar$ Geochronology, elemental and Sr–Nd–Pb isotope geochemistry of the Neogene bimodal volcanism in the Yükselen area, NW Konya (Central Anatolia, Turkey). J African Earth Sci 129: 427–444

Gençoğlu Korkmaz G, Kurt H, Asan K (2021) Classification and Generation of the Enclaves in Karapınar–Karacadağ Volcanic Rocks (Central Anatolia). Turk J Geosci 2: 30–46

Gençoğlu Korkmaz G, Kurt H, Asan K, Leybourne M (2022). Ar-Ar Geochronology and Sr–Nd–Pb–O Isotopic

Systematics of the Post-collisional Karapınar–Karacadağ Volcanic Complex (Central Anatolia, Turkey): An alternative model for orogenic geochemical signature in sodic alkali basalts. J Geosci 67: 53–69

Gertisser R, Keller J (2003) Trace Element and Sr, Nd, Pb and O Isotope Variations in Medium-K and High-K Volcanic Rocks from Merapi Volcano, Central Java, Indonesia: Evidence for the Involvement of Subducted Sediments in Sunda Arc Magma Genesis. J Petrol 44, 3: 457–489

Gleeson MLM, Gibson SA (2019) Crustal controls on apparent mantle pyroxenite signals in ocean-island basalts. Geology 47: 321–324

Göğüş OH, Pysklywec RN, Şengör A, Gün E (2017) Drip tectonics and the enigmatic uplift of the Central Anatolian Plateau. Nat Commun 8: 1–9

Green D, Ringwood A (1967) The genesis of basaltic magmas. Contrib Mineral Petrol 15: 103–190

Guo Z, Wilson M, Zhang M, Cheng Z, Zhang L (2015) Post-collisional ultrapotassic mafic magmatism in South Tibet: products of partial melting of pyroxenite in the mantle wedge induced by roll-back and delamination of the subducted Indian continental lithosphere Slab. J Petrol 56: 1365–1406

Gurenko A, Hoernle K, Sobolev A, Hauff F, Schmincke H (2010) Source components of the Gran Canaria (Canary Islands) shield stage magmas: Evidence from olivine composition and Sr–Nd–Pb isotopes. Contrib Mineral Petrol 159: 689–702

Harris C, Le Roux P, Cochrane R, Martin L, Duncan A, S. Marsh J, P. le Roex A, Class C (2015) The oxygen isotope composition of Karoo and Etendeka picrites: High $\delta^{18}O$ mantle or crustal contamination? Contrib Mineral Petrol 170: 1–24

Herzberg C (2006) Petrology and thermal structure of the Hawaiian plume from Mauna Kea volcano. Nature 444: 605–609

Herzberg C (2011) Identification of Source Lithology in the Hawaiian and Canary Islands: Implications for Origins. J Petrol 52, 113–146

Herzberg C, Asimow PD, Arndt N, Niu Y, Lesher C, Fitton J, Saunders A (2007) Temperatures in ambient mantle and plumes: Constraints from basalts, picrites, and komatiites. Geochem Geophys Geosyst: 8: 2007Q02006, DOI:10.1029/2006GC001390

Herzberg C, Cabral RA, Jackson MG, Vidito C, Day JMD, Hauri EH (2014) Phantom Archean crust in Mangaia hotspot lavas and the meaning of heterogeneous mantle. Earth Planet Sci Lett 396: 97–106

Hirschmann MM, Stolper EM (1996) A possible role for garnet pyroxenite in the origin of the "garnet signature" in MORB. Contrib Mineral Petrol 124: 185–208

Hofmann AW (1988) Chemical differentiation of the Earth: the relationship between mantle, continental crust, and oceanic crust. Earth Planet Sci Lett 90: 297–314

Howarth G, Harris C (2017) Discriminating between pyroxenite and peridotite sources for continental flood basalts (CFB) in southern Africa using olivine chemistry. Earth Planet Sci Lett 475: 143–151

Howarth GH, Udry A (2017) Trace elements in olivine and the petrogenesis of the intermediate, olivine-phyric shergottite NWA 10170. Meteorit. Planet Sci 52: 391–409

Hu JH, Song XY, He HL, Zheng WQ, Yu SY, Chen LM, Lai CK (2018) Constraints of texture and composition of clinopyroxene phenocrysts of Holocene volcanic rocks on a magmatic plumbing system beneath Tengchong, SW China. J Asian Earth Sci 154: 342–353

Humphreys MCS, Blundy JD, Sparks RSJ (2006) Magma Evolution and Open-System Processes at Shiveluch Volcano: Insights from Phenocryst Zoning. J Petrol 47: 2303–2334

Innocenti F, Mazzuoli R, Pasquarè G, Radicati Di Brozolo F, Villari L (1975) The Neogene calcalkaline volcanism of Central Anatolia: geochronological data on Kayseri–Nigde area. Geol Mag 112: 349–360

Irvine T, Baragar WRA (1971) A Guide to the Chemical Classification of the Common Volcanic Rocks. Can J Earth Sci 8: 523–548

Ito G, Mahoney JJ (2005) Flow and melting of a heterogeneous mantle: 1. Method and importance to the geochemistry of ocean island and mid-ocean ridge basalts. Earth Planet Sci Lett 230: 29–46

Jankovics MÉ, Sági T, Astbury RL, Petrelli M, Kiss B, Ubide T, Németh K, Ntaflos T, Harangi S (2019) Olivine major and trace element compositions coupled with spinel chemistry to unravel the magmatic systems feeding monogenetic basaltic volcanoes. J Volcanol Geotherm Res 369: 203–223

Jeffcoate AB, Elliott T, Kasemann SA, Ionov D, Cooper K, Brooker R (2007) Li isotope fractionation in peridotites and mafic melts. Geochim Cosmochim Acta 71: 202–218

Kamenetsky VS, Maas R, Kamenetsky MB, Yaxley GM, Ehrig K, Zellmer GF, Bindeman IN, Sobolev AV, Kuzmin DV, Ivanov AV, Woodhead J, Schilling J-G (2017) Multiple mantle sources of continental magmatism: Insights from "high-Ti" picrites of Karoo and other large igneous provinces. Chem Geol 455: 22–31

Keller J (1974) Quaternary Maar Volcanism near Karapinar in Central Anatolia. Bull Volcanol 38: 378–396

Kheirkhah M, Neill I, Allen MB (2015) Petrogenesis of OIB-like basaltic volcanic rocks in a continental collision zone: Late Cenozoic magmatism of Eastern Iran. J Asian Earth Sci 106: 19–33

Koepke J, Schoenborn S, Oelze M, Wittmann H, Feig ST, Hellebrand E, Boudier F, Schoenberg R (2009) Petrogenesis of crustal wehrlites in the Oman ophiolite: Experiments and natural rocks. Geochem Geophys Geosyst 10: Q10002, DOI: 10.1029/2009GC002488

Kogiso T, Hirschmann MM, Pertermann M (2004a) High-pressure Partial Melting of Mafic Lithologies in the Mantle. J Petrol 45: 2407–2422

Kogiso T, Hirschmann MM, Reiners PW (2004b) Length scales of mantle heterogeneities and their relationship to ocean island basalt geochemistry. Geochim Cosmochim Acta 68: 345–360

Kürkçüoğlu B, Sen E, Aydar E, Gourgaud A, Gündoğdu N (1998) Geochemical approach to magmatic evolution of Mt. Erciyes stratovolcano Central Anatolia, Turkey. J Volcanol Geotherm Res 85: 473–494

Kürkcüoğlu B, Yürür MT (2022) Source constraints for the young basaltic rocks from the northernmost end of Cappadocian region, Turkey: Melting evidence from peridotite and pyroxenite source domains. Geochemistry 82: 125838, DOI:10.1016/j.chemer.2021.125838

Kurt H, Gençoğlu Korkmaz G, Asan K (2019) Textural and Mineral Chemistry Data Related to the Karapinar-Karacadag Volcanic Complex (Konya-Central Anatolia). In: Doronzo D, Schingaro E, Armstrong-Altrin J, Zoheir B (eds) Petrogenesis and Exploration of the Earth's Interior. CAJG 2018. Advances in Science, Technology & Innovation. Springer, Cham, pp 45–47

Le Bas MJ, Le Maitre RW, Streckeisen A, Zanettin BA (1986) A Chemical Classification of Volcanic Rocks Based on the Total Alkali-Silica Diagram. J Petrol 127: 745–750.

Le Roux V, Lee C-T, Turner S (2010) Zn/Fe systematics in mafic and ultramafic systems: Implications for detecting major element heterogeneities in the Earth's mantle. Geochim Cosmochim Acta 74: 2779–2796

Le Roux V, Dasgupta R, Lee CTA (2011) Mineralogical heterogeneities in the Earth's mantle: Constraints from Mn, Co, Ni and Zn partitioning during partial melting. Earth Planet Sci Lett 307: 395–408

Li YQ, Ma CQ, Robinson PT, Zhou Q, Liu ML (2015) Recycling of oceanic crust from a stagnant slab in the mantle transition zone: Evidence from Cenozoic continental basalts in Zhejiang Province, SE China. Lithos 230: 146–165

Liu Z, Shea JJ, Foley SF, Bussweiler Y, Rohrbach A, Klemme S, Berndt J (2021) Clarifying source assemblages and metasomatic agents for basaltic rocks in eastern Australia using olivine phenocryst compositions. Lithos 390–391: 106122.

Lofgren G (1974) An experimental study of plagioclase crystal morphology; isothermal crystallization. Amer J Sci 274: 243–273

Mann CP (2010) Magma chamber dynamics at Soufrière Hills volcano, Montserrat. McGill University, PhD thesis, 1–220

Matzen AK, Wood BJ, Baker MB, Stolper EM (2017) The roles of pyroxenite and peridotite in the mantle sources of oceanic basalts. Nat Geosci 10: 530–535

Mckenzie D, Bickle M (1988) The volume and composition of melt generated by extension of the lithosphere. J Petrol 29: 625–679

McKenzie D, O'Nions RK (1991) Partial melt distributions from inversion of rare earth element concentrations. J Petrol 32: 1021–1091

McNab F, Ball PW, Hoggard MJ, White NJ (2018) Neogene uplift and magmatism of Anatolia: insights from drainage analysis and basaltic geochemistry. Geochem Geophys Geosyst 19: 175–213

Morgan JP (2001) Thermodynamics of pressure-release melting of a veined plum pudding mantle. Geochem Geophys Geosyst 2: 2000GC000049, DOI: 10.1029/2000GC000049

Nakagawa M, Wada K, Wood CP (2002) Mixed magmas, mush chambers, and eruption triggers: evidence from zoned clinopyroxene phenocrysts in andesitic scoria from the 1995 eruptions of Ruapehu Volcano, New Zealand. J Petrol 43: 2279–2303

Nakamura N (1974) Determination of REE, Ba, Fe, Mg, Na and K in carbonaceous and ordinary chondrites. Geochim Cosmochim Acta 38: 757–775

Neumann ER, Wulff-Pedersen E, Simonsen S, Pearson N, Martí J, Mitjavila J (1999) Evidence for fractional crystallization of periodically refilled magma chambers in Tenerife, Canary Islands. J Petrol 40: 1089–1123

Notsu K, Fujitani T, Ui T, Matsuda J, Ercan T (1995) Geochemical features of collision-related volcanic-rocks in central and eastern Anatolia, Turkey. J Volcanol Geotherm Res 64: 171–191

Okay AI, Tüysüz O (1999) Tethyan sutures of northern Turkey. In: Durand B, Jolivet L, Hovarth F, Séranne M (eds) The Mediterranean Basins: Tertiary Extension within the Alpine Orogen. Geol Soc London Spec Publ vol 156, pp 475–515

Pasquarè G, Poli S, Vezzoli L, Zanchi A (1988) Continental arc volcanism and tectonic setting in Central Anatolia, Turkey. Tectonophysics 146: 217–230

Paton C, Hellstrom J, Paul B, Woodhead J, Hergt J (2011) Iolite: freeware for the visualisation and processing of mass spectrometric data. J Anal At Spectrom 26: 2508–2518

Pearce J (1996) A user's guide to basalt discrimination diagrams. In: Wyman DA (ed) Trace Element Geochemistry of Volcanic Rocks: Applications for Massive sulphide Exploration. Geol Assoc Canad Short Course Notes 12: 79–113

Pecerillo A (2005) Plio-Quaternary Volcanism in Italy. Petrology, Geochemistry, Geodynamics. Springer, Berlin, Heidelberg, pp 1–370

Pecerillo A, Taylor S (1976) Geochemistry of Eocene calc-alkaline volcanic rocks from the Kastamonu area, northern Turkey. Contrib Mineral Petrol 58: 63–81

Petrelli M, Perugini D, Alagna KE, Poli G, Peccerillo A (2008) Spatially resolved and bulk trace element analy-

sis by laser ablation-inductively coupled plasma-mass spectrometry (LA-ICP-MS). Period Mineral 77: 1–21

Petrelli M, El Omari K, Le Guer Y, Perugini D (2016a) Effects of chaotic advection on the timescales of cooling and crystallization of magma bodies at mid-crustal levels. Geochem Geophys Geosyst 17: 425–441

Petrelli M, Laeger K, Perugini D (2016b) High spatial resolution trace element determination of geological samples by laser ablation quadrupole plasma mass spectrometry: implications for glass analysis in volcanic products. Geosci J 20: 851–863

Pilet S, Baker MB, Stolper EM (2008) Metasomatized lithosphere and the origin of alkaline lavas. Science 320: 916–919

Platzman ES, Tapirdamaz C, Sanver M (1998) Neogene anticlockwise rotation of central Anatolia (Turkey): preliminary palaeomagnetic and geochronological results. Tectonophysics 299: 175–189

Putirka K (2008) Clinopyroxene thermobarometers. Accessed at http://www.fresnostate.edu/csm/ees/faculty-staff/putirka.html#downloads

Reid MR, Schleiffarth WK, Cosca MA, Delph JR, Blichert-Toft J, Cooper KM (2017) Shallow melting of MORB-like mantle under hot continental lithosphere, Central Anatolia. Geochem Geophys Geosyst 18: 1866–1888

Reid M, Delph J, Cosca M, Schleiffarth W, Kuşcu GG (2019) Melt equilibration depths as sensors of lithospheric thickness during Eurasia-Arabia collision and the uplift of the Anatolian Plateau. Geology 47: 943–947

Schleiffarth WK, Darin MH, Reid MR, Umhoefer PJ (2018) Dynamics of episodic Late Cretaceous–Cenozoic magmatism across Central to Eastern Anatolia: New insights from an extensive geochronology compilation. Geosphere 14: 1990–2008

Şengör AMC, Yilmaz Y (1981) Tethyan evolution of Turkey: A plate tectonic approach. Tectonophysics 75: 181–241

Şengör Amc, Özeren S, Genç T, Zor E (2003) East Anatolian high plateau as a mantle-supported, north–south shortened domal structure. Geophys Res Lett 30: 8045

Sheldrick T, Barry T, Hinsbergen D, Kempton P (2018) Constraining lithospheric removal and asthenospheric input to melts in Central Asia: A geochemical study of Triassic to Cretaceous magmatic rocks in the Gobi Altai (Mongolia). Lithos 296: 297–315

Søager N, Portnyagin M, Hoernle K, Martin Holm P, Folkmar H, Garbe-Schönberg D (2015) Olivine major and trace element compositions ins Payenia basalts, Argentina: evidence for pyroxenite-peridotite melt mixing in a back-arc setting. J Petrol 56: 1495–1518

Sobolev AV, Hofmann AW, Sobolev SV, Nikogosian IK (2005) An olivine-free mantle source of Hawaiian shield basalts. Nature 434: 590–597

Sobolev AV, Hofmann AW, Kuzmin DV, Yaxley GM, Arndt NT, Chung SL, Danyushevsky LV, Elliott T, Frey FA, Garcia MO, Gurenko AA, Kamenetsky VS, Kerr AC, Krivolutskaya NA, Matvienkov VV, Nikogosian IK, Rocholl A, Sigurdsson IA, Sushchevskaya NM, Teklay M (2007) The amount of recycled crust in sources of mantle-derived melts. Science 316: 412–417

Stroncik N, Klügel A, Hansteen T (2009) The magmatic plumbing system beneath El Hierro (Canary Islands): Constraints from phenocrysts and naturally quenched basaltic glasses in submarine rocks. Contrib Mineral Petrol 157: 593–607

Temel A, Gundogdu, M.N., Gourgaud, A. (1998) Petrological and geochemical characteristics of Cenozoic high-K calc-alkaline volcanism in Konya, Central Anatolia, Turkey. J Volcanol Geotherm Res 85: 327–354

Thompson RN, Gibson SA (2000) Transient high temperatures in mantle plume heads inferred from magnesian olivines in Phanerozoic picrites. Nature 407: 502–504

Toprak V (1998) Vent distribution and its relation to regional tectonics, Cappadocian Volcanics, Turkey. J Volcanol Geotherm Res 85: 55–67

Uslular G, Gençalioğlu-Kuşcu G (2019) Mantle source heterogeneity in monogenetic basaltic systems: a case study of Eğrikuyu monogenetic field (Central Anatolia, Turkey). Geosphere 15: 1–29

Uslular G, Gençalioğlu-Kuşcu G, Arcasoy A (2015) Size-distribution of scoria cones within the Eğrikuyu Monogenetic Field (Central Anatolia, Turkey). J Volcanol Geotherm Res 301: 56–65

van Hinsbergen DJ, Kaymakci N, Spakman W, Torsvik TH (2010) Reconciling the geological history of western Turkey with plate circuits and mantle tomography. Earth Planet Sci Lett 297: 674–686

Wang B, Shu L, Faure M, Jahn B-M, Cluzel D, Charvet J, Chung -L, Meffre S (2011) Paleozoic tectonics of the southern Chinese Tianshan: insights from structural, chronological and geochemical studies of the Heiyingshan ophiolitic mélange (NW China). Tectonophysics 497: 85–104

Weaver BL (1991) The origin of ocean island basalt end-member compositions: trace element and isotopic constraints. Earth Planet Sci Lett 104: 381–397

Yang ZF, Zhou JH (2013) Can we identify source lithology of basalt? Sci Rep 3: 1856, DOI: 10.1038/srep01856

Yaxley GM (2000) Experimental study of the phase and melting relations of homogeneous basalt+ peridotite mixtures and implications for the petrogenesis of flood basalts. Contrib Mineral Petrol 139: 326–338

Ying JF, Zhou XH, Zhang LC, Wang F (2010) Geochronological framework of Mesozoic volcanic rocks in the Great Xing'an Range, NE China, and their geodynamic implications. J Asian Earth Sci 39: 786–793

Zhang GL, Zong CL, Yin XB, Li H (2012) Geochemical constraints on a mixed pyroxenite–peridotite source for East Pacific Rise basalts. Chem Geol 330–331: 176–187

Zhang Y, Yuan C, Sun M, Chen M, Hong L, Li J, Lin Z (2019) Recycled oceanic crust in the form of pyroxenite contributing to the Cenozoic continental basalts in central Asia: new perspectives from olivine chemistry and whole-rock B–Mo isotopes. Contrib Mineral Petrol 174: 1–23